

A Sequential Approach to the Management of Posterior Glenoid Defects in RSA

Angulated BIO Versus Multiple Bioresorbable Pinning-Assisted Structural Bone-Grafting

Shinji Imai, MD, PhD

Investigation performed at the Department of Orthopaedic Surgery, Shiga University of Medical Science, Otsu, Shiga, Japan

Background: Large posterior glenoid defects pose problems in reverse shoulder arthroplasty (RSA). We have adopted a sequential approach to the management of posterior glenoid defects using asymmetrical reaming, the placement of a ring graft around the central peg (bony-increased offset, or BIO), or structural bone-grafting, depending on the amount of glenoid retroversion. Furthermore, we have devised multiple bioresorbable pinning (MBP)-assisted bone-grafting, in which as many bioresorbable pins as required are inserted, from whichever aspects of the graft necessary, to achieve initial stability.

Methods: We reviewed 52 shoulders with posterior glenoid defects undergoing RSA between 2014 and 2019 (mean follow-up, 4.8 years; range, 2 to 6 years). Twenty (38.5%) of the shoulders had glenoid retroversion of $<15^\circ$ and were treated by asymmetrical reaming (Group A), 19 (36.5%) of the shoulders had retroversion of $\geq 15^\circ$ to $<30^\circ$ and were treated with asymmetrical reaming combined with angulated ring graft around the central peg (Group B), and 13 (25.0%) of the shoulders had retroversion of $\geq 30^\circ$ and were treated with MBP-assisted bone-grafting (Group C).

Results: Mean version correction was $10.6^\circ \pm 4.3^\circ$ in Group A, $20.7^\circ \pm 8.8^\circ$ in Group B, and $33.8^\circ \pm 9.6^\circ$ in Group C. The mean postoperative active anterior elevation was $138.3^\circ \pm 12.3^\circ$, $128.3^\circ \pm 12.3^\circ$, and $126.5^\circ \pm 15.3^\circ$ in the 3 groups, respectively. The mean postoperative Constant score was 66.8 ± 14.6 , 62.2 ± 13.5 , and 61.7 ± 16.7 , respectively. The mean preoperative active anterior elevation was significantly higher in Group A than in Group C ($p = 0.037$). The full or partial graft-incorporation rate ($\geq 25\%$ of original size) was 89.5% in Group B and 100% in Group C. One glenoid fracture and 1 case of transient brachial plexus palsy occurred in Group B (10.5%), and 1 acromion fracture and 2 cases of transient brachial plexus palsy occurred in Group C (23.1%).

Conclusions: The results of the present sequential approach to management of posterior glenoid defects by the 3 modalities were acceptable. The present MBP-assisted bone-grafting procedure is an effective treatment for cases of shoulder arthropathy with severe posterior glenoid defects. Angulated ring grafting around the central peg may yield equally acceptable results, although its graft-incorporation rate requires further follow-up.

Level of Evidence: Therapeutic Level III. See Instructions for Authors for a complete description of levels of evidence.

Reverse shoulder arthroplasty (RSA) is an accepted treatment for glenohumeral arthritis combined with glenoid bone loss¹⁻³. Posterior glenoid defects have been associated with inferior results in primary shoulder arthroplasty^{4,5}. In the past, a large glenoid defect was even considered a contraindication to the implantation of a glenoid component⁴. To date, 3 ways of managing the glenoid defect have been accepted. The first is asymmetrical reaming, the second is the use of baseplates augmented with precast metal, and the third is bone-grafting.

Surgeons first corrected glenoid retroversion by asymmetrical reaming, i.e., reaming of anterior cortical bone⁶. Good clinical results have been reported for asymmetrical reaming when correcting retroversion of $<10^\circ$ by removing <5 mm of glenoid bone⁷. However, asymmetrical reaming compromises the glenoid bone quality when retroversion exceeds 10° ⁸.

Bone-grafting has also been used to compensate for glenoid retroversion. Two distinct techniques have been described. One is to place a ring-shaped bone graft around the central peg^{9,10}. This technique has been called “bony-increased offset

Disclosure: The **Disclosure of Potential Conflicts of Interest** form is provided with the online version of the article (<http://links.lww.com/JBJSOA/A328>).

Copyright © 2021 The Authors. Published by The Journal of Bone and Joint Surgery, Incorporated. All rights reserved. This is an open-access article distributed under the terms of the [Creative Commons Attribution-Non Commercial-No Derivatives License 4.0](https://creativecommons.org/licenses/by-nc-nd/4.0/) (CCBY-NC-ND), where it is permissible to download and share the work provided it is properly cited. The work cannot be changed in any way or used commercially without permission from the journal.

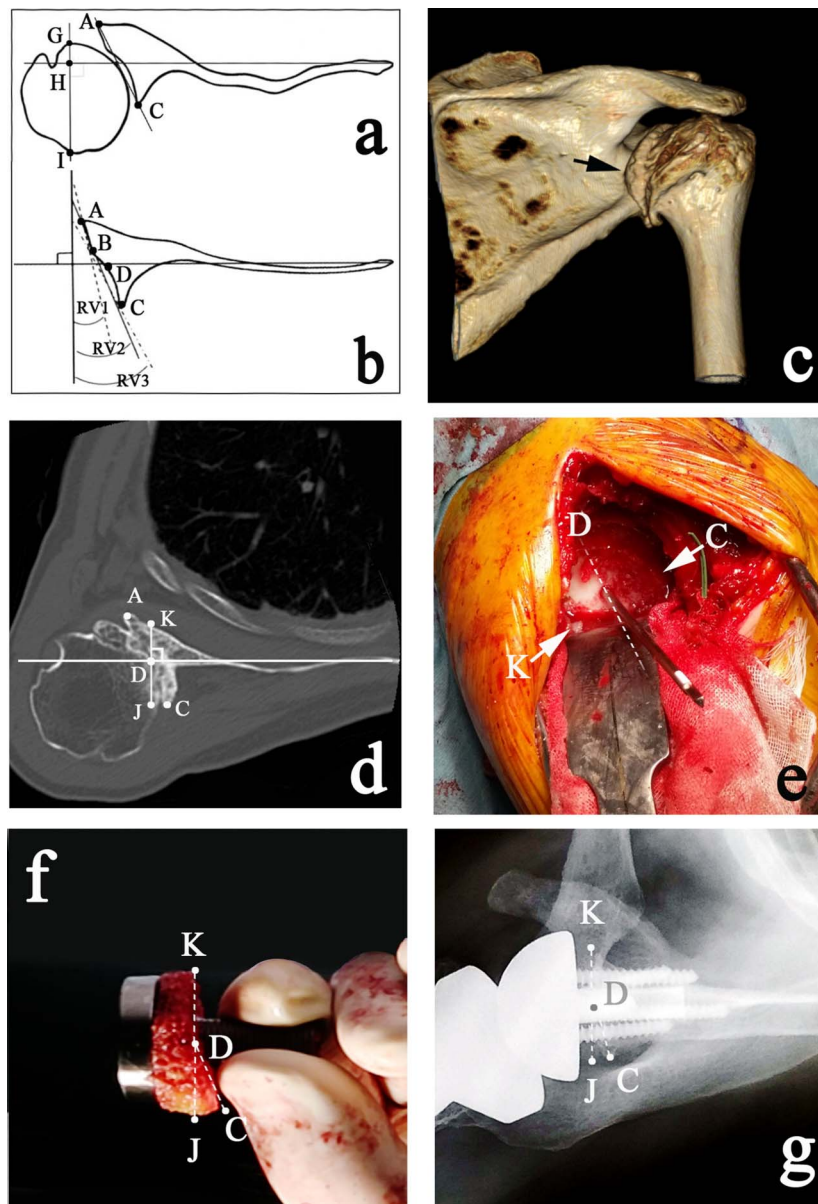


Fig. 1

Figs. 1-A through 1-G Angulated bony-increased offset (BIO) RSA for a posterior glenoid defect. **Fig. 1-A** Diagram illustrating preoperative CT measurements. The Friedman line is defined as a line drawn from the medial tip of the scapula through the center of the glenoid¹³. A = the anterior ridge of the glenoid, and C = the posterior ridge of the glenoid. Another line is drawn perpendicular to the Friedman line such that it passes through the widest portion of the humeral head (line G-I). Posterior subluxation is defined as the percentage of the humeral head that lies posterior to the Friedman line (HI/GI). The subluxation (HI/GI) in this example is 75.2%. **Fig. 1-B** Measurement of version. Line A-C represents the intermediate glenoid; the retroversion of the intermediate glenoid (RV2 angle) is the angle between line A-C and a line perpendicular to the Friedman line. B = the anterior ridge of the glenoid defect. Line B-C represents the posterior neoglenoid; the retroversion of the neoglenoid (RV3 angle) is the angle between line B-C and a line perpendicular to the Friedman line. RV1 is the original retroversion. **Fig. 1-C** Three-dimensional CT image demonstrating Favard E1 (concentric) glenoid erosion with a posterior osteophyte (arrow). This deformity is B2, E1, indicating a uniplanar biconcave deformity, i.e., posteriorly biconcave but not superiorly or inferiorly migrated. **Fig. 1-D** Line K-J represents the presumed asymmetrically reamed plane, with point C being the nonreamed posterior ridge. D = the center of the glenoid. **Fig. 1-E** An intraoperative view immediately after asymmetrical reaming. The anterior side the dotted line (D) is reamed, with the arrow (K) indicating the anterior ridge of the reamed glenoid. The posterior side of the dotted line (D) remains nonreamed, with the arrow (C) indicating the posterior ridge of the glenoid. **Fig. 1-F** The shape of an angulated BIO graft formulated from preoperative CT drawings. The posterior ridge of the BIO graft (C) is fitted to the posterior ridge of the nonreamed glenoid ridge (Fig. 1-E, C). The anterior ridge of the BIO graft (K) is fitted to the anterior ridge of the reamed glenoid (Fig. 1-E, K). **Fig. 1-G** Postoperative axial radiograph. Definitions of the points are the same as those in Figure 1-F.

TABLE I Etiologies and Characterization of Deformities*

	Group			Total
	A	B	C	
Etiologies				
CTA	17	14	2	33
OA	3	5	9	17
RA	0	0	2	2
Total	20	19	13	52
Walch classification				
B2	16	13	8	37
B3	4	6	5	15
Total	20	19	13	52
Favard classification				
E0	7	4	1	12
E1	10	4	2	16
E2	3	8	8	19
E3	0	3	2	5
Total	20	19	13	52

*The values are given as the number of patients. CTA = cuff-tear arthropathy, OA = osteoarthritis, and RA = post-rheumatic arthropathy. Walch classification¹⁵: Type B2 = retroverted glenoid with posterior rim erosion, and Type B3 = glenoid retroversion of >25° regardless of erosion. Favard classification¹⁶: E0 = no erosion with humeral head superior migration, E1 = central erosion, E2 = superior erosion, and E3 = more severe central and superior erosion.

(BIO).¹¹ Although BIO adequately addresses the excessive medialization when applied in combination with asymmetrical reaming, the initial concept was not to correct retroversion. To compensate for glenoid retroversion by BIO, Boileau et al. have further developed “angulated BIO,” in which one end of the ring graft is obliquely cut according to the version or inclination of the deformed glenoid¹². For severe deformity (>25°), a 3-dimensional (3D) virtual model is preoperatively prepared to formulate the shape of the ring graft as well as to serve as a template for placement of the guidewire and central peg¹².

Another option is to fill the glenoid defect with structural bone graft. Although good outcomes have been reported with structural humeral-head autograft¹⁻³, difficulties with bone-grafting have been described, stemming from the difficulty of establishing initial stability^{1-3,11,12}. To this end, we have devised a multiple bioresorbable pinning (MBP)-assisted procedure, which allows as many bioresorbable pins as required to be inserted, from whichever aspects of the graft necessary, to achieve initial stability.

The purpose of this study was to establish a sequential approach to the management of posterior glenoid defects. We hypothesized that glenoid bone deformity is better treated by a sequential approach according to the severity of retroversion, i.e., the use of asymmetrical reaming for mild deformity (<15°), asymmetrical reaming with a handmade angulated BIO graft for

moderate deformity (≥15° to <30°), and structural bone-grafting using the MBP procedure for severe deformity (≥30°).

Materials and Methods

Patients

We retrospectively investigated the demographic, clinical, and radiographic features of patients who underwent RSA for arthropathies with posterior glenoid defects (Figs. 1-A and 1-B). The inclusion criteria were based on preoperative computed tomography (CT). No patients were excluded from the study because of the absence of preoperative CT. Preoperative glenoid retroversion angles were measured in all cases using axial-plane 2D CT according to the modified Friedman technique¹³. The Friedman line is defined as a line drawn from the medial tip of the scapula through the center of the glenoid¹³. In Figure 1, “A” is defined as the anterior ridge of the glenoid, and “C” is designated as the posterior ridge of the glenoid (Fig. 1-A). Line A-C represents the intermediate glenoid. In cases of monoconcave retroversion, RV2 (retroversion of the intermediate glenoid) represents the pathological version angle. “B” is designated as the anterior ridge of the glenoid defect (Fig. 1-B). Line B-C represents the posterior neoglenoid; RV3 (retroversion of the neoglenoid) is the angle between line B-C and a line perpendicular to the Friedman line. In cases of biconcave retroversion, RV3 (retroversion of the posterior eroded glenoid) represents the pathological version angle (Fig. 1-B)¹⁴.

Patients were evaluated and scored preoperatively and at the latest follow-up using the American Shoulder and Elbow Surgeons (ASES) score, the Constant score, the Simple Shoulder Test (SST), and a visual analog scale (VAS) for shoulder pain (0 to 10), and active anterior elevation and external rotation were measured.

Surgical Procedures

Patients underwent 1 of 3 different therapeutic modalities, depending on retroversion angles. A superolateral approach was used in all 52 primary RSAs, with the Aequalis Reversed shoulder arthroplasty (Tornier) prosthesis used in 34 shoulders, and the Delta Xtend (DePuy Orthopaedics) used in 18 shoulders.

Group A

Twenty patients had mild retroversion (<15°) and underwent RSA with asymmetrical reaming (Group A) (Table I). The limit of 15° of retroversion was set by a computer simulation (Image-Pro; Media Cybernetics), which demonstrated that asymmetrical reaming of a glenoid with 10° of retroversion results in 5-mm medialization of the joint line, whereas asymmetric reaming of a glenoid with 15° of retroversion results in 7-mm medialization. The author made the decision to neutralize the 7-mm medialized glenoid facet by adding 7 mm of BIO. Thus, 7-mm medialization was considered to be the limit, over which an RSA should be performed by compensating for the medialization by the BIO technique (Group B).

Group B

Nineteen patients had moderate retroversion (≥15° to <30°) and underwent RSA with asymmetrical reaming with angulated

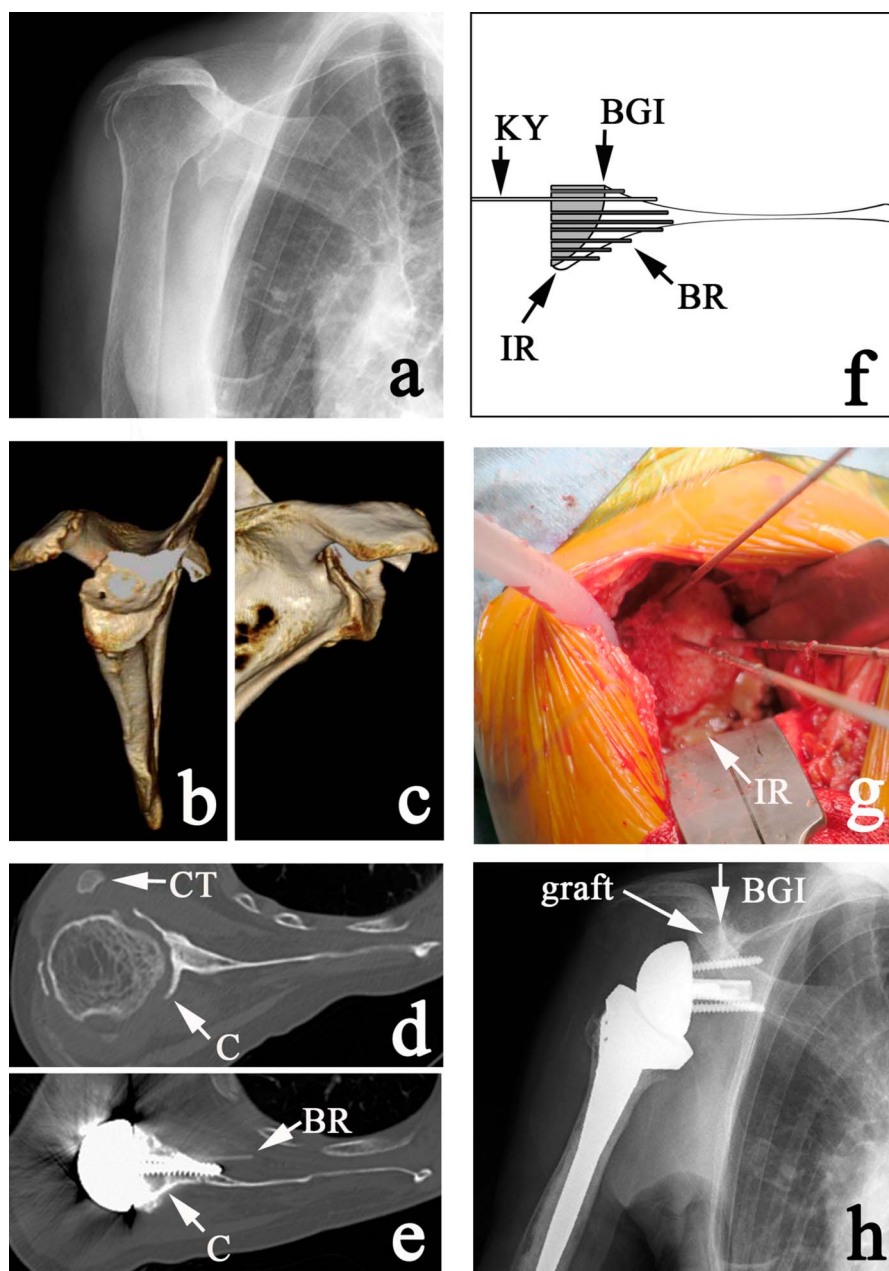


Fig. 2

Figs. 2-A through 2-H Multiple bioresorbable pinning (MBP)-assisted structural humeral bone graft. **Fig. 2-A** Preoperative anteroposterior radiograph. **Fig. 2-B** Preoperative 3D CT demonstrating massive E2 (superior) glenoid erosion. **Fig. 2-C** Preoperative 3D CT demonstrating massive B2 (posterior biconcave) glenoid erosion. This deformity is B2, E2, indicating a multiplanar biconcave deformity. **Fig. 2-D** Preoperative axial CT. The Friedman line is defined on the slice immediately below the coracoid tip (CT). Point C = the posterior ridge of glenoid erosion. **Fig. 2-E** Postoperative axial CT demonstrating the structural humeral graft aligned to the posterior ridge of the glenoid (C). A bioresorbable pin (BR) was accidentally pushed into the subscapularis muscle by an interfering screw. **Fig. 2-F** Diagram illustrating grafting of the humeral graft. KY = Kirschner wire, BGI = bone-graft interface, BR = bioresorbable pin, and IR = inferior ridge. **Fig. 2-G** Intraoperative view of the humeral structural graft aligned to the inferior ridge (IR). **Fig. 2-H** Postoperative anteroposterior radiograph. The surgeon always tries to align the graft to the bone-graft interface (BGI).

BIO (Group B) (Table I). The limit of 30° of retroversion was set by the computer-based imaging analysis so that $>50\%$ of the surface of the BIO graft may contact the reamed facet (Fig. 1-D, line K-D; Fig. 1-E, reamed facet: K side of line D).

In creating a handmade angulated BIO graft, preoperative CT is important for determining the graft thickness and angulation of the graft (Figs. 1-D, 1-F, and 1-G, angle J-D-C). The nonreamed posterior defect (Fig. 1-E, nonreamed facet: C side of

TABLE II Patient Demographics and Operative Details*

	Group			P Value	
	A	B	C	A vs. C	B vs. C
No. of patients	20	19	13		
Age (yr)	71.3 ± 5.3	73.2 ± 4.2	71.7 ± 4.9		
Female (no. [%])	11 (57.9)	13 (65.0)	9 (69.0)		
Preop. retroversion (deg)	12.6 ± 2.7	24.9 ± 4.8	36.7 ± 5.6	0.036	0.062
Version correction (deg)	10.6 ± 4.3	20.7 ± 8.8	33.8 ± 9.6	<0.001	0.042
Preop. β angle (deg)	85.2 ± 7.8	77.3 ± 8.8	70.9 ± 9.7	0.041	0.092
β-angle correction (deg)	2.1 ± 7.8	9.6 ± 5.8	15.6 ± 9.8	0.035	0.085
Graft source	None	Humeral	Humeral		
Type of graft	None	Structural	Structural		

*Age and measurement values are given as the mean and standard deviation.

line D) is fitted to the angulated part of the graft (Figs. 1-D, 1-F, and 1-G, angle J-D-C).

Group C

Thirteen patients had severe retroversion ($\geq 30^\circ$) and under-vent RSA with structural bone-grafting. A structural bone graft is made freehand out of the humeral head to fit the defect (Figs. 2-A through 2-D, Video 1). The graft is aligned posteriorly to the posterior ridge of the glenoid defect (C on Figs. 2-D and 2-E), and inferiorly to the inferior ridge (Figs. 2-F and 2-G, IR). The author always tried to set a structural graft at -5° of version.

After setting the graft, 8 to 10 provisional 1.5-mm Kirschner wires (Fig. 2-F, KY) are inserted and subsequently exchanged for bioresorbable pins (1.5-mm Fixsorb Pin; TEI-JIN) (Figs. 2-E and 2-F, BR). The number of bioresorbable pins can be increased; the maximum number of pins that we have used in the past is 15 for a revision case.

During the MBP procedure, all transient Kirschner wires should penetrate both the graft bone and the scapular bone. Keep “the deepest” Kirschner wire, which reaches the most medial cortical bone of the scapula, as a future guidewire for central peg-hole drilling. It will guide the central peg to the correct position. The author always tried to set the baseplate with no inclination but with 7-mm inferior offset (Fig. 2-H). In many cases, the correction of deformity required not only restoration of version but also of inclination (Figs. 2-B and 2-C, Table II).

Radiographic Evaluations

Postoperative inclination was evaluated by measuring the β angle on a standing true anteroposterior radiograph of the shoulder (Fig. 2-H, Table II), and postoperative version was evaluated by measuring the version angle on a prone axillary radiograph (Fig. 3, Table II)^{15,16}. Version correction was determined on the basis of the difference between measurements on preoperative CT and postoperative radiographs.

Periprosthetic radiolucency was defined as follows: grade 0 = no radiolucent line, grade 1 = incomplete 1-mm line, grade 2 = complete 1-mm line, grade 3 = incomplete 1.5-mm line, grade 4 = complete 1.5-mm line, and grade 5 = complete 2-mm-wide radiolucent line¹⁷.

No cases required revision surgery of the glenoid component for implant loosening. However, a glenoid component was considered to be “at risk” for clinical loosening if there was migration or tilt of the component or glenoid radiolucency of grade 4 or 5¹⁸.

Postoperative graft-bone incorporation was evaluated by axillary radiographs (Fig. 3). Graft incorporation was defined for the purposes of this study as fully incorporated (>75%), partially incorporated (25% to 75%), or not incorporated (<25%) according to the amount of graft remaining on the latest axillary radiographs².

Statistical Analysis

An unpaired Student t test was used to evaluate the significance of the difference between the values of variables. A Pearson chi-square test was applied to evaluate the significance of the difference between expected frequencies and observed frequencies. The level of significance was set at $p < 0.05$.

Source of Funding

There was no external funding source.

Results

Patient Demographic and Preoperative Radiographic Data

Fifty-two patients (19 male and 33 female; mean age [and standard deviation] of 72.5 ± 4.4 years) underwent RSA from 2014 to 2019 for posterior glenoid bone loss and had a minimum follow-up of 2 years (mean, 4.8 years; range, 2 to 6 years) (Table II). The patients underwent 3 different treatment modalities according to glenoid retroversion; mean retroversion was $12.6^\circ \pm 2.7^\circ$ in Group A, $24.9^\circ \pm 4.8^\circ$ in Group B, and $36.7^\circ \pm 5.6^\circ$ in Group C (Table II).

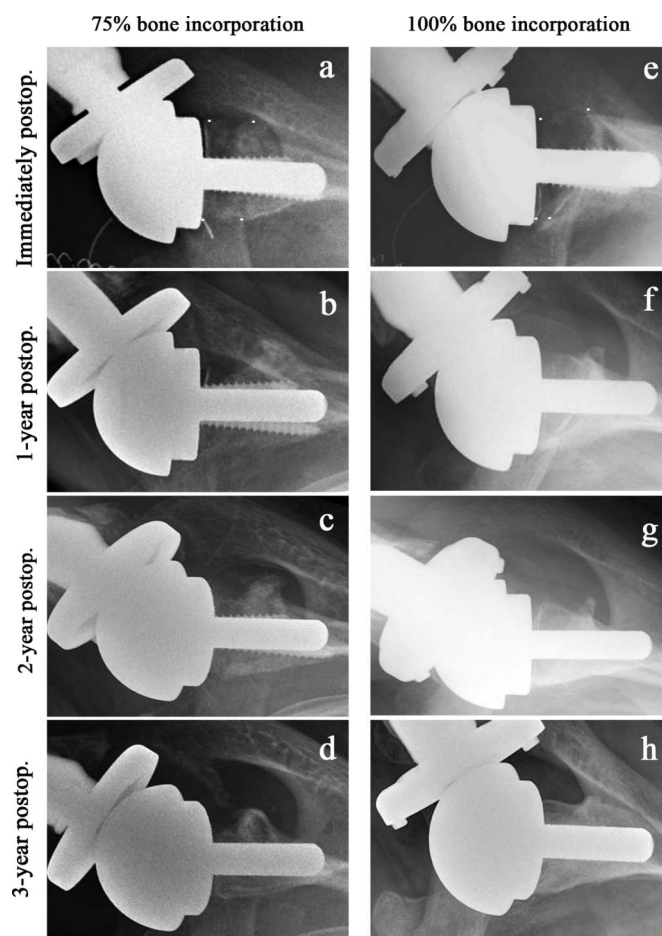


Fig. 3

Figs. 3-A through 3-D Axillary radiographs showing an MBP-assisted graft that finally reached 75% bone incorporation. **Fig. 3-A** Immediately after surgery; the 4 small dots represent the original shape of the graft. **Fig. 3-B** One year postoperatively, showing attenuated radiodensity of the graft and disappearance of a portion. **Fig. 3-C** Two years postoperatively, showing increasing radiodensity of the bone graft. **Fig. 3-D** Three years postoperatively, showing discernible cortical bone and cancellous bone, indicating active remodeling and vascularization of the graft. However, the graft was only 75% of the original size, and turned out to be the smallest of those in group C. **Figs. 3-E through 3-H** Axillary radiographs showing an MBP-assisted graft that finally reached 100% bone incorporation. **Fig. 3-E** Immediately after surgery; the 4 small dots represent the original shape of the graft. **Fig. 3-F** One year postoperatively, showing increased radiodensity of the graft. Trabecular bone has not yet appeared. **Fig. 3-G** Two years postoperatively, showing discernible cortical bone and cancellous bone, indicating active remodeling and vascularization of the graft. **Fig. 3-H** Three years postoperatively, showing further increases in graft size and radiodensity, indicating maturation of the bone structure in response to its mechanical environment; graft incorporation was 100%.

Group A consisted of 20 patients with mild retroversion ($<15^\circ$), who underwent RSA with asymmetrical reaming. Seventeen patients in this group had cuff-tear arthropathy (CTA), and 3 had primary osteoarthritis (OA) (Table I).

Group B consisted of 19 patients with moderate retroversion ($\geq 15^\circ$ to $<30^\circ$), who underwent RSA with asymmetrical reaming combined with a handmade angulated BIO graft. In this group, 14 patients had CTA and 5 had primary OA (Table I); the etiological backgrounds were similar to those of group A (Table I).

Group C consisted of 13 patients with severe retroversion ($\geq 30^\circ$), who underwent RSA with MBP-assisted structural bone-grafting (Table I). The etiological background for Group C was distinct from those of groups A and B, with 2 in Group C having CTA, 9 having OA, and 2 having post-rheumatic arthropathy (Table I). Types of glenoid version and inclination were classified according to the Walch classification¹⁵ and Favard classification¹⁶ (Table I).

Clinical and Radiographic Results

All 52 of the patients improved with respect to the VAS for pain ($p < 0.001$) and postoperative active anterior elevation ($p < 0.001$) and external rotation ($p < 0.001$). The mean postoperative active anterior elevation in Group A was $138.3^\circ \pm 12.3^\circ$; in Group B, $128.3^\circ \pm 12.3^\circ$; and in Group C, $126.5^\circ \pm 15.3^\circ$ (Table III). Mean preoperative active anterior elevation and postoperative external rotation were significantly greater in Group A compared with Group C ($p = 0.037$ and $p = 0.041$, respectively) (Table III). The mean postoperative Constant score was 66.8 ± 14.6 in Group A, 62.2 ± 13.5 in Group B, and 61.7 ± 16.7 in Group C (Table III). Moderate-to-good results were obtained for postoperative ASES and SST scores in all groups, with no significant differences between the groups (Table III).

The mean version correction was $10.6^\circ \pm 4.3^\circ$ in Group A, $20.7^\circ \pm 8.8^\circ$ in Group B, and $33.8^\circ \pm 9.6^\circ$ in Group C. The mean version correction in group C was significantly greater than that in Group B ($p = 0.042$) and that in group A ($p < 0.001$) (Table II). Periprosthetic radiolucency of grade 1 or 2 was seen in 7 cases in Group A, 6 cases in Group B, and 3 cases in Group C (Table III). In addition, more severe periprosthetic radiolucency placing the shoulder “at risk for glenoid loosening” was seen in 2 patients in Group B (Table III). No revision procedure was undertaken in these 2 cases with periprosthetic radiolucency “at risk for glenoid loosening,” as the patients’ pain and functional impairments were minimal.

Graft incorporation was graded according to the size of the remaining grafts evaluated on the latest axial radiographs². Nine cases in Group B and 13 cases in Group C were considered to have full incorporation ($>75\%$ of original size), while 8 in Group B and none in Group C were considered to have partial incorporation ($\geq 25\%$ to 75% of original size) (Table III). Graft resorption, i.e., nonincorporation ($<25\%$ of original graft size), was seen in 2 patients in Group B and in no patient in Group C (Table III).

Since the MBP-assisted bone grafts undergo extensive remodeling until reaching their final size, the final size on an axial radiograph must be evaluated at least after the third postoperative year (Fig. 3). The full or partial graft-incorporation rate ($\geq 25\%$ of original size) was 89.5% for group B and 100% for group C,

TABLE III Clinical and Radiographic Outcomes*

	Group			P Value	
	A	B	C	A vs. C	B vs. C
VAS for pain†	8.9 ± 1.3	7.9 ± 2.7	7.9 ± 3.7	0.072	0.089
Preop. active AE† (deg)	68.3 ± 9.3	53.2 ± 10.2	47.7 ± 13.9	0.037	0.088
Postop. active AE† (deg)	138.3 ± 12.3	128.3 ± 12.3	126.5 ± 15.3	0.062	0.189
Postop. ER† (deg)	22.6 ± 7.7	19.9 ± 10.8	18.7 ± 7.6	0.041	0.078
Postop. ASES score†	72.8 ± 12.7	68.6 ± 10.7	70.7 ± 10.7	0.092	0.169
Postop. Constant score†	66.8 ± 14.6	62.2 ± 13.5	61.7 ± 16.7	0.062	0.085
Postop. SST†	8.8 ± 2.3	7.8 ± 3.7	7.9 ± 2.7	0.098	0.269
Periprosthetic radiolucency of grade 1 or 2 ¹⁷	N = 7	N = 6	N = 3	0.169	0.599
Periprosthetic radiolucency of grade 4 or 5; at risk for clinical loosening	N = 0	N = 2	N = 0	0.136	0.251
Fully incorporated (>75% of original size)		N = 9	N = 13		<0.001
Partially incorporated (25% to 75%)		N = 8	N = 0		0.0069
Not incorporated (<25%)		N = 2	N = 0		0.22
Full-incorporation rate (>75%)		47.4% (9/19)	100% (13/13)		0.0016
Full + partial-incorporation rate (≥25%)		89.5% (9+8)/19	100% (13/13)		0.132

*AE = anterior elevation, and ER = external rotation. †The values are given as the mean and standard deviation.

whereas the full-incorporation rate (>75% of the original size) was 47.4% and 100% in Groups B and C, respectively (Table III).

Regarding complications, 6 (30%) of the shoulders in Group A had scapular notching. One glenoid fracture and 1 case of transient brachial plexus palsy occurred in Group B (10.5%), and 1 acromion fracture and 2 cases of transient brachial plexus palsy occurred in Group C (23.1%).

Discussion

Posterior glenoid defects pose difficulties in RSA. Numerous strategies, such as asymmetrical reaming⁸, placement of an angulated BIO graft⁹⁻¹¹, and structural bone-grafting¹⁻³, have been described. However, it is difficult to definitively recommend one of the 3 strategies over another. Using a sequential approach to manage posterior glenoid defects in RSA, the present study aimed to report specifically on the results of asymmetrical reaming (Group A), angulated BIO (Group B), and MBP-assisted structural bone-grafting (Group C).

The present study demonstrated that RSA with asymmetrical reaming (Group A) was associated with significant improvements in active anterior elevation, external rotation, pain, and functional scores ($p < 0.001$ for all), despite considerable occurrence of scapular notching (30%) when applied for glenoid retroversion of $<15^\circ$.

Larger glenoid defects were addressed by 2 distinct techniques: angulated BIO (Group B) and MBP-assisted structural bone-grafting (Group C). RSA with angulated BIO resulted in significant improvements in active anterior elevation, external rotation, pain, and functional scores ($p < 0.001$ for all), despite a lower rate of full (>75%) graft incorporation (47.4%). One

glenoid fracture and 1 case of transient brachial plexus palsy occurred in this group.

The MBP-assisted structural bone-grafting (Group C) was associated with significant improvements in active anterior elevation, external rotation, pain, and functional scores ($p < 0.001$ for all) with a good graft-incorporation rate (Table III). The better graft-incorporation rate of this group may have resulted from the multiple 1.5-mm-diameter Kirschner wire holes, reaching as deep as the most medial cortical bone of the scapula (Fig. 2-F). In a standard situation, a total of 15 to 20 transient Kirschner wires are inserted—not at the same time, but one set of 5 to 7 wires after another. The most stable wires, usually 8 to 10 of them, are replaced by the bioresorbable pins. These multiple bone holes, whether filled or unfilled with the bioresorbable materials, may promote neovascularization and osteoinduction. The long-lasting remodeling of the MBP-assisted grafts (Fig. 3) may underlie good bone incorporation.

Boileau et al. reported outcomes of angulated BIO RSA for the treatment of posterior glenoid defects¹². They developed specially designed instruments to harvest and shape the angulated BIO graft and addressed multiplanar deformity¹².

Correction of multiplanar glenoid deformity is mandatory. Indeed, 17 patients in Group A had concomitant E0 (no erosion, 7 patients) or E1 (concentric erosion, 10 patients) deformities, indicating that 85% (17 of 20) in Group A had uniplanar deformity. In turn, 11 patients in Group B had E2 (superior erosion, 8 patients) or E3 (more severe central and superior erosion, 3 patients) deformities, with the mean preoperative inclination of the glenoid facet, i.e., the β angle, being $77.3^\circ \pm 8.8^\circ$, indicating that Group B had multiplanar deformity.

BIO works very well to address contained defects and medialization of the joint line but may not be suitable for severe peripheral defects. This is the reason why we set the limit for this procedure to $<30^\circ$ of retroversion. We suspect that the observed rate of full graft incorporation (47.4%, Table III) might have fallen further if the procedure had been applied to shoulders with retroversion of $\geq 30^\circ$. Alternatively, structural bone-grafting enables the correction of large multiplanar defects, although it may be complicated by graft failure and subsequent glenoid loosening^{1-3,11,19}. The optimal type of bone-grafting and technique for placement and stabilization remain controversial.

Many authors use Kirschner wires to gain initial stability of the graft. Kirschner wires are not inserted from the baseplate-facing aspect of the graft but from its periphery³, suggesting limited provisional stability. Kirschner wires are then removed after implantation of the baseplate, and a single long screw is applied, penetrating the graft and glenoid³, suggesting that a single screw, or at most 2 screws, must be aimed at a very narrow space between the central post and screws. We believe that the present MBP-assisted structural bone-grafting is a reliable and reproducible technique for otherwise difficult or even impossible glenoid reconstruction.

The radiographic analysis is a study limitation, as preoperative CT was used for preoperative measurements but

radiographs were used for postoperative assessments; inclination and version angles differ between the 2 methods. Another limitation of the study is the heterogeneities resulting from uniplanar or multiplanar deformities and different etiologies. The small sample sizes of the cohort overall and the individual groups are additional limitations of the present study.

The results of the present sequential approach to the management of posterior glenoid defects using the 3 modalities were acceptable. The MBP-assisted bone-grafting procedure is an effective treatment for shoulder arthropathy involving severe posterior glenoid defects. Angulated ring graft around the central peg (i.e., angulated BIO) may yield equally acceptable results, although its graft-incorporation rate requires further follow-up. ■

Shinji Imai, MD, PhD^{1,2}

¹Shiga University of Medical Science Hospital, Otsu, Shiga, Japan

²Department of Orthopaedic Surgery, Shiga University of Medical Science, Otsu, Shiga, Japan

Email: simai@belle.shiga-med.ac.jp

References

- Ernstbrunner L, Werthel JD, Wagner E, Hatta T, Sperling JW, Cofield RH. Glenoid bone grafting in primary reverse total shoulder arthroplasty. *J Shoulder Elbow Surg.* 2017 Aug;26(8):1441-7.
- Jones RB, Wright TW, Zuckerman JD. Reverse total shoulder arthroplasty with structural bone grafting of large glenoid defects. *J Shoulder Elbow Surg.* 2016 Sep;25(9):1425-32.
- Tashjian RZ, Granger E, Chalmers PN. Structural glenoid grafting during primary reverse total shoulder arthroplasty using humeral head autograft. *J Shoulder Elbow Surg.* 2018 Jan;27(1):e1-8.
- Cofield RH, Edgerton BC. Total shoulder arthroplasty: complications and revision surgery. *Instr Course Lect.* 1990;39:449-62.
- Iannotti JP, Frangiamore SJ. Fate of large structural allograft for treatment of severe uncontained glenoid bone deficiency. *J Shoulder Elbow Surg.* 2012 Jun;21(6):765-71.
- Magosch P, Habermeyer P, Lichtenberg S, Tauber M, Gohlke F, Mauch F, Boehm D, Loew M, Zeifang F, Pötzel W. [Results from the German shoulder- and elbow arthroplasty register (SEPR) : Anatomic or reverse shoulder arthroplasty in B2-glenoids?]. *Orthopade.* 2017 Dec;46(12):1063-72. German.
- Chin PC, Hachadorian ME, Pulido PA, Munro ML, Meric G, Hoenecke HR Jr. Outcomes of anatomic shoulder arthroplasty in primary osteoarthritis in type B glenoids. *J Shoulder Elbow Surg.* 2015 Dec;24(12):1888-93.
- Chen X, Reddy AS, Kontaxis A, Choi DS, Wright T, Dines DM, Warren RF, Berhouet J, Gulotta LV. Version correction via eccentric reaming compromises remaining bone quality in B2 glenoids: a computational study. *Clin Orthop Relat Res.* 2017 Dec;475(12):3090-9.
- Garofalo R, Brody F, Castagna A, Ceccarelli E, Krishnan SG. Reverse shoulder arthroplasty with glenoid bone grafting for anterior glenoid rim fracture associated with glenohumeral dislocation and proximal humerus fracture. *Orthop Traumatol Surg Res.* 2016 Dec;102(8):989-94.
- Seidl AJ, Williams GR, Boileau P. Challenges in reverse shoulder arthroplasty: addressing glenoid bone loss. *Orthopedics.* 2016 Jan-Feb;39(1):14-23.
- Boileau P, Moineau G, Roussanne Y, O'Shea K. Bony Increased Offset-Reversed Shoulder Arthroplasty (BIO-RSA). *JBJS Essent Surg Tech.* 2017 Dec 27;7(4):e37.
- Boileau P, Morin-Salvo N, Gaudi MO, Seeto BL, Chalmers PN, Holzer N, Walch G. Angled BIO-RSA (bony-increased offset-reverse shoulder arthroplasty): a solution for the management of glenoid bone loss and erosion. *J Shoulder Elbow Surg.* 2017 Dec;26(12):2133-42.
- Friedman RJ, Hawthorne KB, Genez BM. The use of computerized tomography in the measurement of glenoid version. *J Bone Joint Surg Am.* 1992 Aug;74(7):1032-7.
- Rouleau DM, Kidder JF, Pons-Villanueva J, Dynamidis S, Defranco M, Walch G. Glenoid version: how to measure it? Validity of different methods in two-dimensional computed tomography scans. *J Shoulder Elbow Surg.* 2010 Dec;19(8):1230-7.
- Walch G, Badet R, Boulahia A, Khoury A. Morphologic study of the glenoid in primary glenohumeral osteoarthritis. *J Arthroplasty.* 1999 Sep;14(6):756-60.
- Sirveaux F, Favard L, Oudet D, Huquet D, Walch G, Molé D. Grammont inverted total shoulder arthroplasty in the treatment of glenohumeral osteoarthritis with massive rupture of the cuff. Results of a multicentre study of 80 shoulders. *J Bone Joint Surg Br.* 2004 Apr;86(3):388-95.
- Sperling JW, Cofield RH, Rowland CM. Neer hemiarthroplasty and Neer total shoulder arthroplasty in patients fifty years old or less. Long-term results. *J Bone Joint Surg Am.* 1998 Apr;80(4):464-73.
- Mileti J, Boardman ND 3rd, Sperling JW, Cofield RH, Torchia ME, O'driscoll SW, Rowland CM. Radiographic analysis of polyethylene glenoid components using modern cementing techniques. *J Shoulder Elbow Surg.* 2004 Sep-Oct;13(5):492-8.
- Wagner E, Houdek MT, Griffith T, Elhassan BT, Sanchez-Sotelo J, Sperling JW, Cofield RH. Glenoid Bone-Grafting in Revision to a Reverse Total Shoulder Arthroplasty. *J Bone Joint Surg Am.* 2015 Oct 21;97(20):1653-60.